International Journal of Pharmacognosy

PLEUROTUS OSTREATUS POLYSACCHARIDE INDUCES GO/G1 CELL CYCLE ARREST AND APOPTOSIS IN EHRLICH ASCITES CARCINOMA CELL LINE

P. K. Moyen Uddin [* 1], Jane O'Sullivan [2], Mohammad Sayful Islam [3], Mohammad Shahangir Biswas [4], Lubatul Arbia [5], Lutfa Akther [6], Rumana Pervin [7] and Matiar Rahman [7]

Institute of Biological Science 1, Rajshahi University, Bangladesh.
Department of Anaesthesiology and Critical Care [2], Tallaght University Hospital, Dublin, Ireland.
Department of Pharmacy [3], Mawlana Bhashani Science and Technology University, Tangail, Bangladesh.
Department of Biochemistry and Biotechnology [4], School of Biomedical Science, Khwaja Yunus Ali Unversity, Enayetpur, Sirajgonj-6751, Bangladesh.
Department of Biochemistry & Molecular Biology [5], Primeasia University, Dhaka, Bangladesh.
Dhaka Medical College and Hospital [6], Dhaka, Bangladesh.
Department of Biochemistry & Molecular Biology [7], University of Rajshahi, Rajshahi, Bangladesh.

ABSTRACT: In this study, *Pleurotus ostreatus* polysaccharide (POP) is isolated, refined, structurally analysed, and its anticancer properties are investigated. Polysaccharide yield was 6.27%, purified via DEAE-52 and Sephadex S-300 chromatography, with a molecular weight of 154649.8 Da. Structural analysis through FT-IR, HPLC, GC-MS, and NMR revealed POP as a homopolysaccharide composed of D-glucose units, featuring $(1\rightarrow6)$-α-D-Glcp backbone with O-6 branches and T-α-D-Glcp terminations. These findings contribute to understanding the biological potential of POP. POP's antitumor activity study showed that, with an IC_{50} of 121.801 µg/mL, it was highly cytotoxic to EAC cell types, supported by LDH release analysis. POP inhibited cell migration, invasion, and colony formation, indicating its potential as an anti-cancer agent. Analysis using flow cytometry showed that POP induced apoptosis, which raised the expression of Bax and Caspase-9 while decreasing the expression of Bcl-2. DNA fragmentation assay showed characteristic laddering pattern, confirming apoptosis-mediated DNA degradation. Furthermore, alterations in the expression of the proteins p53, Cyclin D, and Cdk4 were linked with POP-induced cell cycle arrest in the G0/G1 phase. In conclusion, this study highlights the potential of *Pleurotus ostreatus* polysaccharides (POP) as an anti-cancer agent, demonstrating significant cytotoxicity against Ehrlich Ascites Carcinoma cells and elucidating its structural and apoptotic mechanisms of action. This study marks a breakthrough, suggesting *Pleurotus ostreatus* polysaccharides (POP) as potential health-food or medicinal agents, offering notable defense against human cancer.

INTRODUCTION: Cancer mortality worldwide raises significant global health concerns [1].

The global count of cancer-related deaths stands at approximately 9.96 million, highlighting its widespread impact [2]. The continued importance of cancer as a major health issue can be attributed, in part, to cancer cells releasing antiapoptotic factors as the disease progresses [3]. The diversity of cancer subtypes limits the treatment landscape, necessitating unique therapeutic approaches for each.

Despite chemotherapy and radiotherapy being standard treatments, they often fall short of patient expectations. This underscores the urgency of exploring alternative cancer therapies. Many cultures have a history of using herbal remedies to combat cancer, as certain plants contain numerous anti-cancer compounds that are relevant to modern drug development [4]. Polysaccharides from different sources have been identified for their potential anti-cancer activities [5, 6].

These polysaccharides' possible physiological roles, including hepatoprotective [9], antioxidative [7], and anticancer [8] activities, have drawn a lot of attention. Studies have particularly associated mushroom-derived biologically active compounds, primarily polysaccharides, with anti-cancer properties [10-14]. *Pleurotus* species, commonly referred to as oyster mushrooms, represent a diverse group of edible fungi cultivated worldwide [15]. These mushrooms are valued for their excellent food quality, offering a rich source of nutrients and flavors. Among the *Pleurotus* species, *Pleurotus ostreatus,* known as the oyster mushroom, holds particular significance as a popular nutritional supplement with purported health benefits, including potential cancer risk reduction [16-18]. Emerging research has highlighted the therapeutic potential of polysaccharides extracted from various parts of different *Pleurotus* species, such as their mycelia and fruit bodies [18, 19].

These studies have yielded promising results, suggesting that polysaccharides isolated from these mushrooms have the potential to inhibit the growth of different kinds of cancer, offering potential avenues for therapeutic intervention [20-21]. Despite these advancements, there remains a significant gap in understanding the specific molecular mechanisms underlying the antitumor effects of *P. ostreatus* polysaccharides. The intricate chemical composition of *P. ostreatus* polysaccharides has not been fully elucidated, hindering a comprehensive understanding of their therapeutic potential. Additionally, the precise molecular pathways through which these polysaccharides exert their antitumor activity remain poorly characterized, necessitating further investigation. Previous research has indicated that polysaccharides isolated from *Pleurotus ostreatus* exhibit anti-tumor properties [22]. However, in

Bangladesh, no studies have explored the anti-tumor effects of *Pleurotus ostreatus* polysaccharide (POP) on Ehrlich Ascites Carcinoma (EAC) cells. In order to provide a solid scientific foundation for the study of polysaccharides and their potential use in medicine, this project aims to investigate the possible anticancer characteristics of POP utilising *in-vitro* models of EAC cells. The results of this investigation support POP's potential effectiveness as a promising cancer therapy.

MATERIALS AND METHODS:

Chemicals and Reagents: The experimental materials DEAE-cellulose 52 and Sephadex S-300 were obtained from Whatman Co. in Maidstone, Kent, UK and Pharmacia Co. in Sweden, respectively. T-series dextrans was obtained from Amersham Pharmacia in Uppsala, Sweden, and was essential for certain assays. Sigma-Aldrich, with its headquarters located in St. Louis, Missouri, USA, provided the solvents and reagents, which included dimethyl sulfoxide (DMSO), EDTA, 3-(4,5-Dimethylthiazol-2-yl)-2,5-diphenyltetrazolium bromide (MTT), phenylmethyl-sulfonyl fluoride (PMSF), RNase-A, Tris-HCL, glycine, and propidium iodide (PI). We purchased primary antibodies from BioVision, Inc., located in CA, USA, against Bax (#3331-100), Bcl-2 (#3195-100), and the horseradish peroxidase (HPR)-conjugated goat anti-mouse secondary antibody (#6402-05). Similarly, we purchased monoclonal antibodies to p53 (#2527), cleaved Caspase-9 (#7237), and goat anti-rabbit secondary antibody (#7074S) conjugated with horseradish peroxidase (HPR) from Cell Signalling Technologies, Inc., a Massachusetts, USA-based company. We obtained enhanced chemiluminescence kits which are necessary for detection from Pioneer Technology, Inc., an American company. Known for its high-quality water purification, Millipore's Milli Q-Plus system from Bedford, Massachusetts, USA was used to prepare the deionized water used in all of the experiments. The accuracy and dependability of the experimental results were guaranteed by the use of only the best commercially available grade of chemicals for everything that wasn't specifically stated above.

Methods:

Sample Collection: Fruiting bodies of *Pleurotus ostreatus* were procured from the Mushroom

Development Institute located in Bangladesh. A Scientific Officer at the National Mushroom Development and Extension Centre, situated in Savar, Dhaka-1340, Bangladesh, verified the authenticity of the specimens, bearing registration number SR-0022 (dated March 2, 2018).

Extraction: The procedures outlined in our previously published article [10] were used to extract the polysaccharide from the *Pleurotus ostreatus* (PO) fruiting bodies. To put it briefly, 30 g of dried *Pleurotus ostreatus* powder was extracted for three hours at 90°C with constant stirring using distilled water (at a ratio of 1:30). This procedure successfully eliminated monosaccharides, polyphenols, and pigments dissolved in hot water. The resultant liquid fraction was precipitated using 95% ethanol (at a ratio of 1:3, v/v) for 12 hours at 40°C after being separated by centrifugation at 5000 rpm for 15 minutes at 56°C. After centrifugation (at 4500 rpm for 20 minutes at 40°C) to collect the precipitates, acetone (1:3 v/v, 95%), ether (1:3 v/v, 95%), and ethanol (1:3 v/v, 95%) were used as washing solutions at 40°C. The final precipitate was vacuum-dried to produce the polysaccharide bound to protein (PBP). The total polysaccharide content was measured using the phenol-sulfuric acid method [24], while the total protein content was determined using the Lowry method [23].

Protein free Polysaccharides Isolation: Using the Sevag method, the crude extract of POP (*Pleurotus ostreatus* polysaccharide) was deproteinated [25]. The sample and Sevag reagent were combined at a 2:1 ratio (Chloroform: n-Butanol, 5:1) in accordance with the Sevag principle, and a 2:1 ratio was the ideal ratio for POP to Sevag reagent. The following formula was used to determine the deproteination rate:

$$\text{Deproteination rate (\%)} = [(P_{co} - P_{ca}) / P_{co}] \times 100,$$

Where the pre-deproteinization protein content is denoted by P_{co} and the post-deproteinization protein content by P_{ca}.

After the solution was deproteinized, it was desalinated using hyperfiltration (3 Kda, 5.0 mL/min for 8 hours). The filtrate that was left over was combined with 99.5% ethanol and stored for 24 hours at 40°C. The precipitate was dissolved in

dH2O and then lyophilized in a vacuum freeze dryer to yield the crude polysaccharide, POP, following centrifugation (4000 rpm, 4°C, for 15 minutes).In order to create a standard curve, D-glucose ($C_6H_{12}O_6$) and the following expressions were used to express the standard curve's linearity as well as the POP extraction yield:

$$Y = 0.6932 * X + 0.1772, (R^2 = 0.9902, p < 0.001),$$

Where Y represents the absorbance, and X represents the POP content (mg/mL).

Finally, the POP yield was calculated using the formula:

$$\text{POP yield (\%)} = X_{poly} \text{ (mg)} / W_{mushroom\ power} \times 100$$

Where X represents the POP content (mg), and W represents the weight of the mushroom powder (g).

Purification of Polysaccharides by Chromatographic Methods: Both gel filtration chromatography (GFC) and DEAE-Ion exchange chromatography (IEC) were used as purification techniques to refine the crude polysaccharide (POP) and remove fine particles. First, a step gradient elution was carried out using dH2O, 0.2 M NaCl, and 0.5 M NaCl on a DEAE-52 column (2.6 x 80 cm) loaded with crude POP The phenol-sulfuric acid supplementary method was utilised to measure the carbohydrate content in 5 mL test tubes while maintaining an elution flow rate of 0.8 mL/min. The fractions that contained the most polysaccharides were combined, gathered, and subjected to additional processing via gel filtration chromatography. A Sephadex S-300 column (1.6 x 100 cm) was loaded with the pooled fractions and equilibrated using 0.05 M NaCl. A 24 mL/hr elution flow rate was chosen. After collecting the largest fraction with the highest polysaccharide content, the fraction was desalted using a dialysis membrane with a molecular weight cutoff (MWCO) of 14,000 Da for five days while being dialyzed against ddH2O (Thermo Fisher Scientific). The polysaccharide solution was concentrated and then lyophilized to produce the refined polysaccharide following the dialysis procedure. The polysaccharide was produced in a concentrated and purified form as a result of this purification process, which guaranteed the removal of contaminants.

Relative Molecular Weight Determination using HPLC: Using high performance size exclusion chromatography (HPSEC) on an HPLC system (Shimadzu LC-2010A) outfitted with a size exclusion chromatography (SEC) column, the molecular weight of POP was ascertained. POP (1 mg/mL, 10 µl) was injected into the column, and 0.8 mL/min of ultrapure water was used to elute the sample. By comparing POP to a calibration curve made with Dextran standards (10-2000 kDa), the molecular weight of POP was calculated.

Spectroscopic Analysis of Polysaccharide:
UV-vis Spectroscopic Analysis: A Double Beam UV-visible Light Spectrophotometer from China was used to dissolve POP in distilled water (up to 5%) and perform UV-vis spectroscopy in order to determine the polysaccharide content. The samples were scanned between 200 and 600 nm by the spectrophotometer. Both the protein and carbohydrate contents were ascertained during this analysis.

Monosaccharide Composition: The mono-saccharide content of the polysaccharide was ascertained by hydrolyzing 2M TFA (2 mL) at 120°C for three hours. The hydrolysate was collected and dissolved in ultrapure water (4 mL) following the removal of excess TFA. $NaBH_4$ (40 mg) was added to the mixture and reduced for three hours at 25°C.Each sealed reaction tube was filled with 3 mL of acetic anhydride and 3 mL of pyridine, and they were left at 100°C for an hour. Using the same process, standard monosaccharides (D-Mannose, D-Glucose, and D-Galactose) were made. Using an Agilent 6890GC with a Column HP-5 (30 m x 0.32 mm), the solutions were examined.

Fourier Transform Infrared Analysis (FT-IR): The polysaccharide's organic functional groups were located using the FT-IR method. POP (3 mg) was dried at 40–45°C before being pressed into a 1 mm pellet using KBr powder in preparation for analysis. At 25°C, the spectrometer recorded wavelengths ranging from 4000 to 400 cm-1 with an 8 cm-1 resolution.

Methylation Analysis: POP methylation analysis was carried out using a previously developed protocol, modified slightly as described in reference [26]. Supplementary Method S1 contains specific experimental procedures.

NMR Spectroscopy Analysis: An NMR spectrometer (Bruker AV-400) from Bruker Instrumental Inc. in Billerica, Massachusetts, USA was used to obtain the 1H- and 13C-NMR spectra of POP. At a temperature of 25°C, these measurements were carried out under carefully monitored circumstances. POP was dissolved in D2O before the spectra were recorded, in order to prepare the sample for analysis.

Cell Lines: Cell lines from Ehrlich ascites carcinoma (EAC) were grown. The RPMI-1640 medium, a kind of cell culture medium intended to promote the growth of diverse cell types, was utilised to cultivate these cells.10% foetal calf serum (FCS), a serum made from the blood of foetal calves that provides vital nutrients and growth factors for cell growth, and 1% (v/v) penicillin-streptomycin, which aids in preventing bacterial contamination, were added to the medium as supplements. The environment in which the cells were cultivated was regulated. In particular, the cells were kept at 37°C (98.6°F) in a humidified environment with 5% CO_2 (carbon dioxide). This setting is similar to what would be found in a laboratory for these cells to grow.

Study of the Cytotoxicity of POP
MTT Assay: Polysaccharide, POP was dissolved in DMSO to make a stock solution (1 mg/mL) for the cytotoxicity study, and it was then kept at -20°C until needed. The entire culture medium was used to freshly prepare the working solution.The entire culture medium was used to freshly prepare the working solution. In a 96-well plate, EAC cells were seeded at a density of 5×10^3 cells/well (200 µL) and left for the night at 5% CO_2 and 95% humidity. Following a 24-hour incubation period, the cells were subjected to POP (varying from 25 to 800 µg/mL) and untreated EAC cells as the negative control. After rinsing the cells with 1× PBS, MTT solution was added. The dark blue formazan crystals were dissolved after two hours of incubation, and a microplate reader was used to measure the absorbance at 570 nm. The provided equation was used to calculate cell viability (percentage of control).

% Cell viability = Abs. of treated cells / Abs. of untreated cells × 100

Lactate Dehydrogenase Assay: Using an LDH Cytotoxicity Detection Kit, the membrane integrity of EAC cell lines was evaluated. LDH leakage into the media was used as a marker for cell membrane damage, which included necrotic and apoptotic processes [27, 28].

Cells were exposed to different concentrations of POP for 24 hours using an assay kit from JianchengBioEngineering, China, in accordance with exact manufacturer instructions.

Following this, 100 µL of cell-free supernatant from each well was transferred in triplicate to a 96-well plate, and 100 µL of the LDH reaction mixture was added to each well. Using a microplate reader, the optical density of the final solution was measured at 450 nm after a 3-hour incubation period under standard conditions. This provided detailed insights into the cytotoxic effects of POP on the EAC cell lines.

Study of the Anti-migratory Effect of POP:
Cell Migration Assay: The procedure described by Yarrow [29] was followed when performing the cell scratch wound healing assay. First, 5×10^5 cells per well of 6-well microplates were used to plate EAC cells, which were subsequently incubated for 48 hours at 37°C.After the cell monolayers reached confluence, 200 µL pipette tips were carefully used to create wounds, which led to the formation of 1 mm wide acellular lanes within each well.

The cells were then thoroughly cleaned with PBS to get rid of any remaining cell debris. The cells were then added to a full medium at concentrations of 0 (Control), 1xIC50, 2xIC50, and 3xIC50, either with or without POP. Photographs were taken at two distinct times during the wound closure process: after 0 and 24 hours of incubation in a dark environment. The degree of cell migration was examined using the Image J programme [30]. Using the following formula, the migration inhibition rate was computed as a percentage of the change in scratch closure:

$$\text{Scratch close change (\%)} = (A_{to} - A_{tc}) / A_{to} \times 100$$

Where the corresponding scratch area at 24 hours is denoted by Atc, and the initial scratch area at time 0 is represented by At0.

Cell Invasion Assay: After POP therapy, EAC cell migration was evaluated using a transwell assay (3xIC50). POP-treated cells were cultured in serum-free medium before being inserted into the upper chamber of transwell inserts that were purchased from Corning Costar, a company located in Illinois, USA. The bottom chamber was simultaneously filled with approximately 600 µL of full medium.After a 24-hour incubation period, the cells that remained on the top membrane were carefully scraped out with a cotton swab. After fixing the cells with methanol, they were stained with crystal violet and imaged and counted [31].

Clonogenic Assay: The protocol for the clonogenic assay closely followed that of a prior study [32]. 200 cells per well in six-well plates were seeded with cells in the exponential growth phase that were taken from a stock culture. Following a 12-hour incubation period, the cells were exposed to a concentration of 3xIC50 of POP after the pre-existing growth medium was removed. The plates were then incubated for a full day. After this incubation period, the growth medium was changed every three days, and after seven days of culturing, the colony formation was evaluated. The cells were fixed with a 4.0% paraformaldehyde solution and then stained with a 0.5% crystal violet solution for colony evaluation. Every step of the experimental process was done twice.

DNA Fragmentation Assay: For the first 24 hours of the experiment, EAC cells were cultivated in a controlled setting with particular parameters, such as a temperature of 37°C and 5.0% CO2. After this incubation, the EAC cells were subjected to two different treatments: either 0.1% DMSO or a POP concentration at 3xIC50 for a full day. Following the treatment, the cells were centrifuged for five minutes at 2000 rpm, and the resultant cell pellet was twice cleaned with PBS. The Cayman DNA Laddering assay kit was used, according to the manufacturer's instructions, to evaluate DNA fragmentation. A dry cell pellet was acquired as a result of this process. The dry pellet was then resuspended in 25 µL of Tris EDTA buffer and subjected to an electrophoresis process. In order to separate DNA fragments using a 0.8% agarose gel stained with ethidium bromide at a concentration of 5.0 mg/ml, 10 µL of EAC cell extract and 2 µL of loading buffer had to be combined.

Agarose gel electrophoresis was used for the electrophoresis, which was run for 65 minutes at 75V. By measuring the DNA fragments against a 1 kb DNA ladder (Invitrogen, USA) that was used as a reference marker, the size of the fragments was ascertained. Under UV light, the resultant DNA fragmentations were seen.

Study of Cell Apoptosis: A BD Bioscience, USA, FACS Calibur flow cytometer was used to assess POP-induced apoptosis. After seeding 1x105 cells/well, EAC cells were left to incubate for the entire night. The medium was changed the next day, and cells were exposed to POP (3×IC50) for 48 hours. Following the manufacturer's instructions, the treated cells were harvested, rinsed with PBS, and stained with PI and Annexin V-FITC using an Invitrogen Dead Cell Apoptosis Kit [33]. Cells were examined after being incubated in the dark for 20 minutes.

Cell Cycle Analysis: DNA content was measured to assess the cell cycle phase distribution of EAC cells. After trypsinization, PBS was used to wash the treated and untreated cells. After fixing the cells for an entire night at 4°C in 70% ice-cold ethanol, any remaining ethanol was removed by washing them with PBS. After the cells were resuspended in PBS containing RNAse A (50 µg/mL), 0.5% Triton X-100, and propidium iodide (50 µg/mL), they were incubated for 30 minutes at 37°C in a water bath. Cell cycle distribution at various phases (G0/G1, S, G2/M, and sub-G1) was assessed in cells using a BD Biosciences, USA, FACS Calibur flow cytometer [34].

Analysis of Apoptotic Protein/G_0G_1 phase Expression: POP treatment was applied after plating EAC cells. The cells were lysed in RIPA buffer containing protease inhibitors following three washes with 1× PBS.

Thermo Scientific's Micro BCA Protein Assay kit was used to measure the concentration of protein. Cell lysates were then subjected to SDS-PAGE separation, PVDF membrane transfer, and primary antibody tagging against caspase 9, BAX, Bcl2, cyclin D1, Cdk4, and p53. Following exposure to HRP-conjugated secondary antibodies, the membranes were detected by chemiluminescence using the ChemiDoc detection of chemiluminescence kit from BioRad (Azure Biosystems) [35].

Statistical Analysis: The statistical analysis was conducted using GraphPad Prism. The data is shown as mean ± standard deviation. For statistical comparisons, one-way analysis of variance (ANOVA) was employed. The IC50 value for the effective doses was given.The polysaccharide IC50 values were used to express the effective doses. When $P<0.05$ separated the values, a statistically significant difference was deemed to exist.

RESULTS:

Extraction and Isolation of POP: The hot-water extraction technique was used for POP extraction. Standard D-glucose was used to validate the phenol-sulfuric acid technique. The results showed that D-glucose had a maximum absorbance at 490 nm and that the standard curve had a high degree of linearity at 99.18% ($p<0.001$).

The crude POP fraction contained proteinated polysaccharides, as evidenced by the absorbance at 280 nm. However, after deproteination, no detectable absorbance at 280 nm was observed, indicating that the POP was free from protein. The yield of POP was 6.27%. During ion-exchange chromatography (DEAE-52), two fractions (F1 and F2) were identified, and further purification of POP was achieved using gel filtration.

Molecular Weight Determination: HPLC was chosen as the method to analyze the average molecular weight of POP. By applying HPLC, the mean molecular weight of POP was determined to be 154649.8 Da. The dextran standard curve, which was created using known molecular weights of dextran standards, generated the equation used in this calculation.

The equation used for this estimation was $logMw = -0.2466*X + 1.683$, where X represents the retention time of the sample. The high coefficient of determination ($R^2 = 0.998$) indicated the reliability and accuracy of the estimation.

Monosaccharide Composition: The monosaccharide composition analysis, as illustrated in **Fig. 1A** and **B**, provided valuable insights into the composition of POP.

It was revealed that the predominant monosaccharide present in POP was glucose. This finding led to the significant identification of POP as a typically acidic homopolysaccharide for the first time.

The characterization of POP as such sheds light on its structural properties and potential applications in various fields.
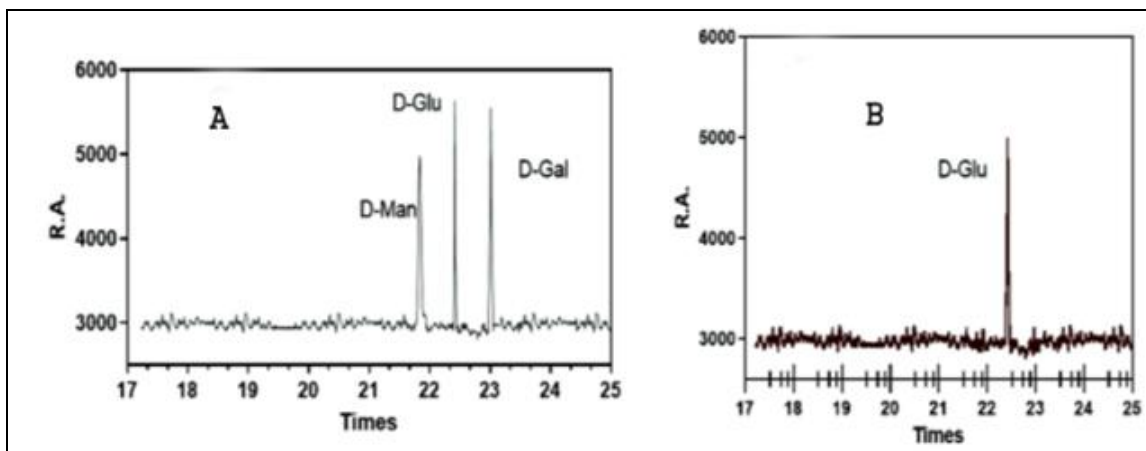

FIG. 1A: STANDARD MONOSACCHARIDE GC SPECTRA. STANDARD MONOSACCHARIDES SUCH AS D-GLUCOSE, D-GALACTOSE, AND D-MANNOSE ARE OFTEN SHOWN IN GAS CHROMATOGRAPHY (GC) SPECTRA WITH RETENTION DURATIONS (R.T.) ON THE X-AXIS AND RELATIVE ABUNDANCE (R.A.) ON THE Y-AXIS. EACH MONOSACCHARIDE APPEARS AS A DISTINCT PEAK AT A CHARACTERISTIC RETENTION TIME, WITH THE PEAK'S HEIGHT OR AREA REPRESENTING ITS RELATIVE ABUNDANCE. THESE SPECTRA ENABLE EASY COMPARISON AND IDENTIFICATION OF MONOSACCHARIDES PRESENT IN A SAMPLE BASED ON THEIR RETENTION TIMES. ADDITIONALLY, THE SHAPE AND WIDTH OF THE PEAKS PROVIDE INSIGHTS INTO THE PURITY AND EFFICIENCY OF THE SEPARATION, WHILE THE REPRODUCIBILITY OF RETENTION TIMES AND PEAK SHAPES ENSURES METHOD RELIABILITY. (B) GC SPECTRA OF POP FRACTION. COMPARING THE GC SPECTRUM TO A STANDARD CURVE (A), WHICH CORRELATES KNOWN CONCENTRATIONS OF D-GLUCOSE WITH THEIR RESPECTIVE SIGNAL RESPONSES, REVEALS A STRONG ALIGNMENT OF PEAKS WITH CONCENTRATIONS ON THE CURVE. THIS ALIGNMENT STRONGLY SUGGESTS A SIGNIFICANT PRESENCE OF D-GLUCOSE WITHIN THE POP FRACTION, INDICATING ITS PREDOMINANT COMPOSITION AS A HOMOPOLYSACCHARIDE. D-Man; D-Mannose, D-Glu; D-Glucose; D-Gal; D-Galactose, and POP; *Pleurotus ostreatus* polysaccharides.

Structural Characterization of Polysaccharide (POP): FT-IR spectroscopy was used to determine the distinctive functional groups of the purified POP, with a wavelength range of 4,000–400 cm-1. POP's FT-IR spectra showed clear peaks at around 3419.8 cm-1, 2924.5 cm-1, and 1615.1 cm-1, which, in turn, corresponded to –OH groups, C–H bonds, and C=O bonds **Fig. 2A**. Furthermore, spectra in the 990–1050 cm-1 region verified the existence of β-glycosidic connections, demonstrating unequivocally that the polysaccharide's main chain is composed of α-D-glucopyranose. Methylation analysis was employed to determine the linkage types between monosaccharide units of POP. Methylated polysaccharide's FT-IR revealed the distinctive peak (C-H) at 1050 cm-1 **Fig. 2B**. Four components were found in the POP according to the methylation study Table 1. Following complete methylation, POP underwent hydrolysis, reduction, and acetylation to yield partially methylated alditol acetate (PMAA), which was then subjected to GC–MS analysis **Table 1**.

Table 1 represents a comprehensive glycosyl linkage analysis of the compound POP, revealing key insights into its structural composition. The major mass fragments, represented by distinct m/z values, provide a detailed fingerprint of specific glycosidic linkages. The linkage-type column specifies the nature and position of these glycosidic bonds, with notations such as "→6)-Glcp-(1→" indicating linkage at the 6th position with a glucose residue. The molar ratio column quantifies the abundance of each linkage type, highlighting variations in their prevalence within the compound. Additionally, the methylated sugars column elucidates the specific modifications present, such

as "2,3,4-tri-O-methyl-D-glucose" and "2,3,4,6-tetra-O-methyl-D-glucose," offering valuable information on the methylation patterns of associated glucose residues. This comprehensive study enhances our knowledge of POP's molecular structure and helps to comprehend its complex glycosylation patterns. The nuclear magnetic resonance (NMR) spectra of POP have been identified for further structural study, as shown in **Fig. 2C** and **2D.**
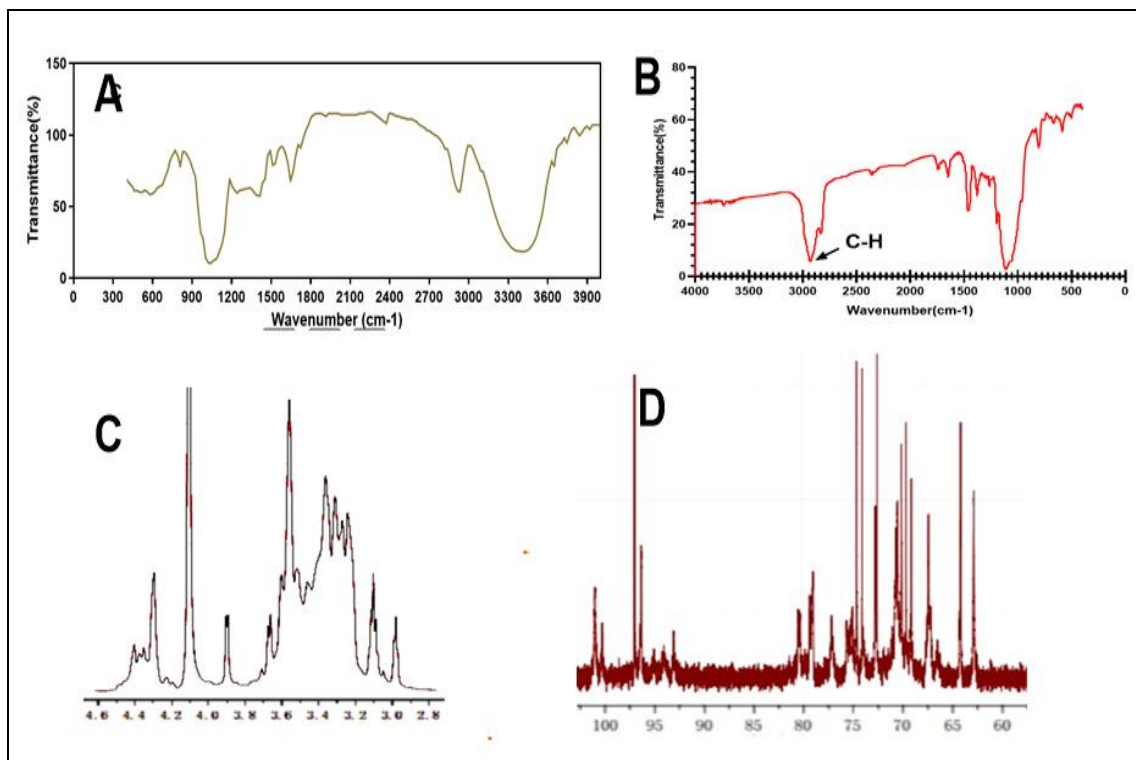

FIG. 2: FT-IR AND NMR ANALYSIS OF POP. (A) THE PURIFIED POP'S DISTINCTIVE FUNCTIONAL GROUPS WERE LOCATED USING FT-IR SPECTROSCOPY BETWEEN 4,000 AND 400 CM^1. THE FOURIER TRANSFORM INFRARED SPECTRA OF THE POLYSACCHARIDE PLEUROTUS OSTREATUS (POP) SHOWED CLEAR PEAKS AT ABOUT 3419.8 CM-1, 2924.5 CM-1, AND 1615.1 CM-1 (FIGURE 2A). THESE PEAKS LINE UP WITH PARTICULAR FUNCTIONAL GROUPS FOUND IN THE STRUCTURE OF POLYSACCHARIDES. THE PRESENCE OF HYDROXYL GROUPS, WHICH ARE INDICATIVE OF CARBOHYDRATES AND POLYSACCHARIDES, IS INDICATED BY THE PEAK AT 3419.8 CM-1. THE STRETCHING VIBRATIONS OF CARBON-HYDROGEN BONDS, WHICH ARE FREQUENTLY PRESENT IN THE ALKYL GROUPS OF CARBOHYDRATES, ARE REPRESENTED BY THE PEAK AT 2924.5 CM-1. MOREOVER, THE STRETCHING VIBRATIONS OF CARBONYL BONDS ARE SHOWN BY THE SIGNAL DETECTED AT 1615.1 CM-1, INDICATING THE PRESENCE OF CARBONYL GROUPS WITHIN THE POLYSACCHARIDE STRUCTURE. FURTHERMORE, MORE EXAMINATION IN THE 990–1050 CM-1 SPECTRUM REGION REVEALED MORE DETAILS ON THE POLYSACCHARIDE'S COMPOSITION. THE RESULTS OF THIS STUDY VERIFIED THE EXISTENCE OF DISTINCTIVE PEAKS LINKED TO B-GLYCOSIDIC CONNECTIONS. THE PRESENCE OF THESE LINKAGES IS INDICATIVE OF THE PRIMARY CHAIN COMPOSITION BEING A-D-GLUCOPYRANOSE UNITS WITHIN THE POLYSACCHARIDE STRUCTURE. (B) METHYLATION ANALYSIS WAS EMPLOYED TO DISCERN THE SPECIFIC LINKAGE TYPES BETWEEN MONOSACCHARIDE UNITS WITHIN THE PLEUROTUS OSTREATUS POLYSACCHARIDE (POP). FOLLOWING METHYLATION, THE FOURIER TRANSFORM INFRARED (FT-IR) SPECTRUM OF THE METHYLATED POLYSACCHARIDE EXHIBITED A DISTINCT PEAK CORRESPONDING TO CARBON-HYDROGEN (C-H) BONDS AT 1050 CM-1 (FIGURE 2B). THIS PEAK, INDICATIVE OF SUCCESSFUL METHYLATION, SIGNIFIES THE INTRODUCTION OF METHYL GROUPS INTO THE POLYSACCHARIDE MOLECULE. THE PRESENCE OF THESE METHYL GROUPS PROVIDES VALUABLE INSIGHTS INTO THE STRUCTURAL ARRANGEMENT AND LINKAGE TYPES PRESENT WITHIN POP. (C-D) ^{1}H-NMR AND ^{13}C-NMR OF POP: THE CHEMICAL SHIFTS OBSERVED IN ^{1}H-NMR SPECTRA FOR PROTONS (H-1 TO H-6) CAN REVEAL INFORMATION ABOUT THE SURROUNDING CHEMICAL GROUPS, NEIGHBORING ATOMS, AND MOLECULAR DYNAMICS. SIMILARLY, THE CHEMICAL SHIFTS OBSERVED IN 13C-NMR SPECTRA FOR CARBONS (C-1 TO C-6) CAN PROVIDE INFORMATION ABOUT THE TYPES OF CARBON ATOMS PRESENT IN THE MOLECULE AND THEIR CONNECTIVITY WITHIN THE MOLECULAR FRAMEWORK.

TABLE 1: GLYCOSYL LINKAGES ANALYSIS OF POP

Major mass fragments (m/z)	Linkage-type	M/R	Methylated sugars (PMAA)
77,112,152,171,204	→6)-Glcp-(1→	4	2,3,4-Me3-Glc
101,112,135,171,204	→6)-Glcp-(1→	1	2,3,4-Me3-Glc
53,77,101,112,135,152	→6)-Glcp-(1→	1	2,3,4-Me3-Glc
53,77,101,112,135,161,171,189,204	Glcp-(1→	1	2,3,4,6-Me4-Glc

Table 1 presents an analysis of glycosyl linkages within POP, presumably a polysaccharide or glycoprotein. The table outlines major mass fragments observed during analysis, corresponding linkage types, molar ratios, and methylated sugars derived from methylation. Notably, the data reveal several linkage types, including →6)-Glcp-(1→ and Glcp-(1→, indicating glucose units with specific linkage patterns. The molar ratios associated with these linkages provide insights into their relative abundance within the structure of POP. Furthermore, the table details partially methylated alditol acetate derivatives, such as Me3-Glc and Me4-Glc, indicating the positions of methylation on glucose units, thus offering valuable information about the structural composition and complexity of POP. PMAA; partially methylated alditol acetate, Glcp; glucose unit, Me3-Glc; methylated glucose; M/R; Molar ratio.

Table 2 represents a comprehensive breakdown of the nuclear magnetic resonance (NMR) spectra of POP. The data encompasses chemical shifts for protons (H-1 to H-6) and carbons (C-1 to C-6) in both hydrogen-1 (^{1}H) and carbon-13 (^{13}C) NMR, offering a detailed glimpse into the electronic environment of specific nuclei within the molecular framework. Each entry, such as "3.61/101.9," corresponds to the chemical shift for a particular proton (e.g., H-1) and its corresponding carbon (e.g., C-1), expressed in parts per million (ppm). These chemical shifts serve as diagnostic signatures, facilitating the correlation of spectral data with specific molecular features and aiding in the elucidation of the compound's structure. The glycosyl residues listed in the last column provide additional valuable information regarding the sugar moieties present in the molecule. Both "beta-D-glucopyranosyl-(1->6)-beta-D-glucopyranose" and "alpha - D – glucopyranosyl - (1->6)- alpha-D-glucopyranose" indicate the glycosidic connections and configurations of the sugar residues. As an example, the notation "alpha-D-glucopyranosyl-(1->6)- alpha- D-glucopyranose" denotes an alpha linkage of the glycosidic bond at position six, linked with an alpha conformation of the D-glucose residue. In contrast, the term "beta-D-glucopyranosyl -(1->6)-beta-D-glucopyranose" designates a beta linkage at position six, where the D-glucose residue is arranged in the beta variant. In summary, the findings from monosaccharide analysis, methylation analysis, and NMR spectroscopy revealed that POP primarily consists of alpha- D -glucopyranosyl - (1->6)-alpha-D-glucopyranose and beta-D-glucopyranosyl-(1->6)-beta-D-glucopyranose units. This structure comprises a backbone of alpha-D-glucopyranosyl-(1->6)-alpha-D-glucopyranose with substitutions at O-6 by beta-D-glucopyranosyl-(1->6)-beta-D-glucopyranose residues. This detailed spectroscopic analysis, integrating ^{1}H and ^{13}C NMR data with glycosyl residue information, offers a robust foundation for the structural characterization of POP. Such precision is pivotal in organic chemistry, enabling a nuanced understanding of molecular architecture and facilitating the delineation of complex molecular structures.

TABLE 2: THE ^{1}H AND ^{13}C RESONANCES OF POP

H-1/C-1	H-2/C-2	H-3/C-3	H-4/C-4	H-5/C-5	H-6/C-6	Glycosyl residues
3.61/102.9	3.92/97.4	3.26/75.8	3.62/65.2	3.38/98.3	3.54/71.9	-6)-α-D-Glcp-(1-
4.45/106.1	4.09/77.9	3.11/86.3	3.09/69.7	3.44/70/5	3.56/66.9	-6)-β-D-Glcp-(1-

Table 2 displays the ^{1}H (proton) and ^{13}C (carbon) chemical shifts for various positions (H-1 to H-6 and C-1 to C-6) within the glycosyl residues of POP (Pleurotus ostreatus polysaccharide), alongside the corresponding glycosyl residues denoted by their linkage type (α-D-Glcp or β-D-Glcp). The chemical shifts provide crucial information about the local chemical environment of the protons and carbons within the glycosyl units, aiding in structural elucidation. The table delineates two distinct glycosyl residues, each characterized by specific chemical shifts for their respective proton and carbon positions. These resonances are fundamental for understanding the configuration and conformation of the glycosidic linkages present in POP, thus contributing to the overall structural characterization of the polysaccharide. POP; Pleurotus ostreatus polysaccharide, α-D-Glcp: α-D-Glucose unit, β-D-Glcp; β-D-Glucose unit.

Anticancer Activity:
The Cytotoxic Effects of POP on EAC Cells: A detailed comparative study was conducted to assess the impact of various concentrations of POP on the viability of EAC cells over a 24-hour period. The results of this investigation were presented in **Fig.**

3A, utilizing the MTT assay to observe cellular viability. The growth curves generated from the data revealed a significant anti-proliferative effect of POP across the entire range of concentrations tested (0–800 µg/mL). Significantly, this effect showed a dose-dependent trend, meaning that EAC cell survival rates were significantly reduced at higher POP concentrations than in untreated cells (p<0.01). Furthermore, the IC_{50} value of POP, which was determined to be 121.801 µg/mL, highlighted its efficacy in preventing the proliferation of EAC cells (p<0.01). An additional assay was conducted to evaluate LDH leakage, providing an additional measure of cytotoxicity, in order to study the inhibitory effect of POP on EAC cell proliferation further. As depicted in **Fig. 3B**, the presence of POP resulted in a substantial increase in LDH leakage from EAC cells (p<0.01), corroborating the findings observed in the MTT assay. This significant elevation in LDH leakage further reinforces the notion that POP exerts potent anti-proliferative effects on EAC cells. These comprehensive findings suggest that POP is a viable therapeutic candidate for the treatment of EAC. Its ability to effectively reduce cell viability and induce cytotoxicity in EAC cells warrants further investigation into its chemical properties and underlying molecular mechanisms responsible for its anticancer effects. Given its high sensitivity to EAC cells demonstrated in this study, exploring the detailed characterization and mode of action of POP could pave the way for its development as a targeted therapy for cancer.
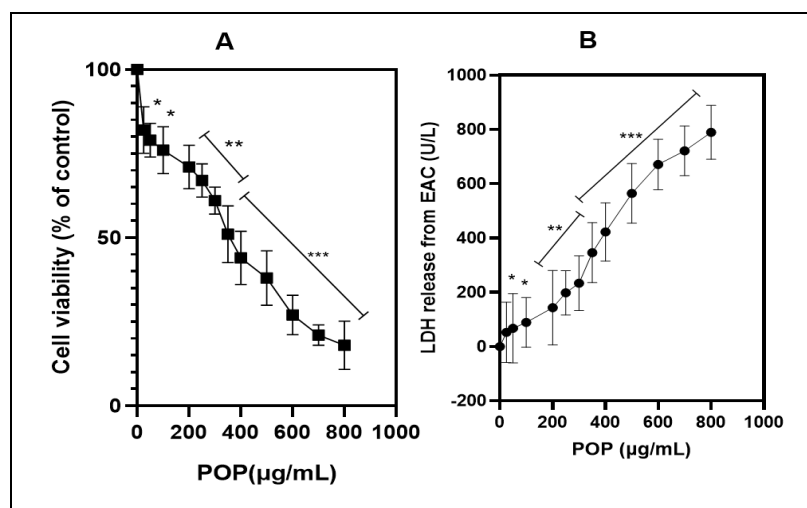

FIG. 3: (A) THE EFFECTS OF POP ON CELLS. THE MTT TEST WAS USED TO ASSESS THE CYTOTOXICITY OF POP ON EAC CELLS. THE DATA'S GROWTH CURVES OFFER A THOROUGH REPRESENTATION OF POP'S EFFECTS AT VARIOUS DOSES, RANGING FROM 0 TO 800 µG/ML. THESE CURVES EFFECTIVELY ILLUSTRATED POP'S ANTI-PROLIFERATIVE ACTION ON EAC (EHRLICH ASCITES CARCINOMA) CELLS. INTERESTINGLY, POP'S INHIBITORY EFFECT ON CELL PROLIFERATION GREW MORE EVIDENT AS ITS CONCENTRATION INCREASED, INDICATING A DOSE-DEPENDENT RELATIONSHIP. (B) LDH RELEASE ANALYSIS. THE SIGNIFICANT INCREASE IN LDH LEAKAGE FURTHER CONFIRMS THE POTENT ANTI-PROLIFERATIVE EFFECTS OF POP ON EAC CELLS, SUGGESTING ITS PROMISE AS A THERAPEUTIC AGENT FOR EAC TREATMENT. THESE FINDINGS, DEMONSTRATING POP'S ABILITY TO MARKEDLY REDUCE CELL VIABILITY AND INDUCE CYTOTOXICITY IN EAC CELLS, UNDERSCORE THE NECESSITY FOR DEEPER EXPLORATION INTO ITS CHEMICAL PROPERTIES AND UNDERLYING MOLECULAR MECHANISMS RESPONSIBLE FOR ITS ANTICANCER PROPERTIES. THE HEIGHTENED SENSITIVITY OF EAC CELLS TO POP, AS EVIDENCED IN THIS STUDY, EMPHASIZES THE IMPORTANCE OF COMPREHENSIVE CHARACTERIZATION AND UNDERSTANDING OF ITS MODE OF ACTION. SUCH INVESTIGATIONS COULD PAVE THE WAY FOR THE TARGETED DEVELOPMENT OF POP AS A CANCER THERAPY. The graph's bars each show the mean ± 95% CI from three separate tests. *p<0.05 and **p<0.01 indicate statistically significant differences from the control group.

Effect of POP on EAC Cells Migration: One of the most important phases of the metastatic cascade is cell migration [36]. Therefore, we investigated how POP affects the migration of Ehrlich Ascites Carcinoma (EAC) cells **Fig. 4A** and **4B**. Our results showed that POP considerably slowed the migration rate of EAC cells relative to untreated cells at concentrations of $1xIC_{50}$, $2xIC_{50}$, and

$3xIC_{50}$. Furthermore, it was observed that there was no statistically significant distinction in the suppression of cell migration between untreated and DMSO-treated cells (data not presented, p-value > 0.05). This finding reveals that DMSO was not responsible for the anti-migration effects that were observed. The results showed that POP at 3xIC50 reduced the number of invasive cells in

Fig. 4C and **4D**. This suggests a significant reduction in EAC cell invasion relative to the untreated group. On the other hand, the colony formation experiment demonstrated that, in comparison to untreated cells (5E and 5F), cells exposed to POP (3xIC50) showed a notable reduction in proliferation.
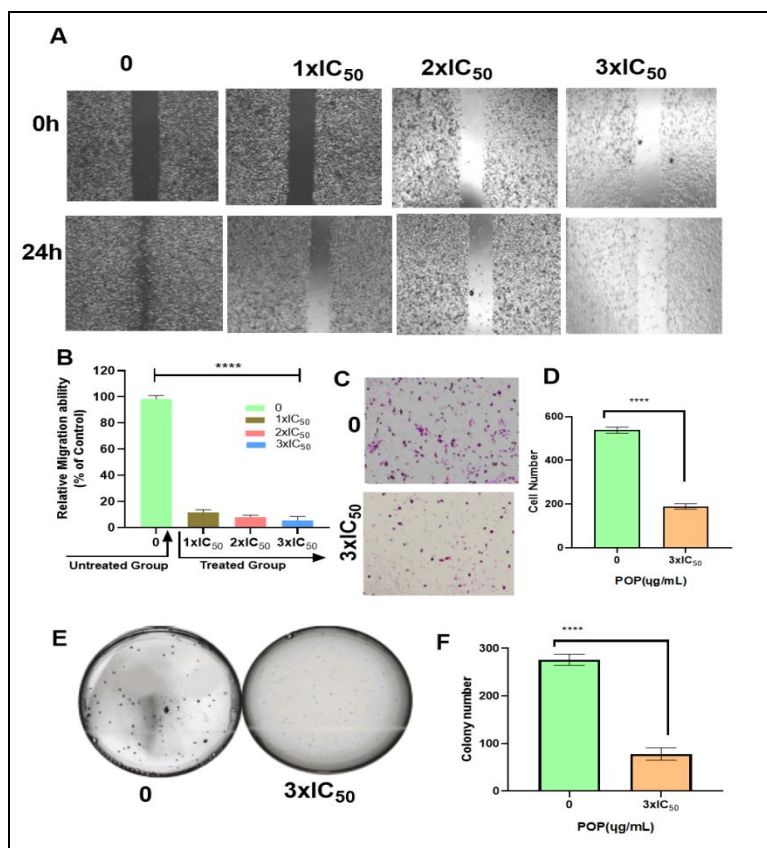

FIG. 4: (A AND B) IN THE EXPERIMENT FOR CELL MIGRATION, POP DRAMATICALLY DECREASED THE MIGRATION RATE OF EAC CELLS IN COMPARISON TO UNTREATED CELLS AT DOSES OF 1XIC50, 2XIC50, AND 3XIC50. POP, AT DOSES EQUIVALENT TO 1XIC50, 2XIC50, AND 3XIC50, SIGNIFICANTLY DECREASED THE MIGRATORY RATE OF EAC CELLS AS COMPARED TO UNTREATED CELLS, ACCORDING TO OUR FINDINGS. FURTHERMORE, A STATISTICAL ANALYSIS REVEALED A NOTEWORTHY DISTINCTION IN THE SUPPRESSION OF CELL MIGRATION BETWEEN CELLS THAT WERE NOT TREATED AND THOSE THAT WERE. THESE FINDINGS DEMONSTRATE THAT POP HAS THE ABILITY TO BLOCK EAC CELLS' ABILITY TO MIGRATE, INDICATING THAT IT MAY BE USED AS A THERAPEUTIC DRUG TO PREVENT CANCER CELLS FROM SPREADING. TARGETED METHODS AGAINST THE PROGRESSION OF CANCER MAY BENEFIT FROM ADDITIONAL RESEARCH INTO THE UNDERLYING PROCESSES BEHIND THE REPORTED ANTI-MIGRATORY IMPACT OF POP. (C AND D) POP CAUSED A REDUCTION IN THE QUANTITY OF INVASIVE CELLS AT 3XIC50. THE RESULTS SHOWED THAT POP TREATMENT AT 3XIC50 SIGNIFICANTLY REDUCED THE NUMBER OF INVASIVE CELLS, AS SEEN IN FIGURES 5C AND 5D. ADDITIONALLY, A STATISTICAL STUDY SHOWED THAT THE SUPPRESSION OF CELL MIGRATION IN TREATED AND UNTREATED CELLS DIFFERED SIGNIFICANTLY. THESE RESULTS HIGHLIGHT THE EFFECTIVENESS OF POP IN REDUCING THE INVASIVENESS OF CANCER CELLS, ESPECIALLY AT HIGHER CONCENTRATIONS. THIS SHOWS THAT POP MAY BE USEFUL AS A THERAPEUTIC AGENT TO STOP THE SPREAD OF CANCER. (E AND F)WHEN COMPARED TO UNTREATED CELLS, CELLS EXPOSED TO POP AT 3XIC50 SHOWED NOTICEABLY SLOWER GROWTH IN THE COLONY FORMATION ASSAY. THE ASSAY DEMONSTRATED A STATISTICALLY SIGNIFICANT (P < 0.05) REDUCTION IN CELL PROLIFERATION BETWEEN POP-TREATED (AT THREE TIMES THE IC50 CONCENTRATION) AND UNTREATED CELLS. THE QUANTITY OF CELLS MOVING INTO THE AREA THAT WAS SCRATCHED, THE NUMBER OF INVASIVE CELLS, AND THE CREATION OF COLONIES ARE ALL DEPICTED IN THE BAR GRAPH. The data are displayed as mean ± sem, and there are n = 4 samples. pop-treated and untreated eac cells differ significantly, as shown by **p < 0.001 and ***p < 0.0001.

Apoptosis Induction on EAC Cells by POP: Apoptosis in numerous cell types is marked by a distinct series of nuclear alterations, ultimately leading to chromatin condensation and fragmentation of the nucleus [37]. The impact of POP on inducing apoptosis in EAC cells was assessed

using flow cytometry. Following a 24-hour POP treatment, EAC cells were ready for cell cycle phase analysis. The percentages of living cells, early-phase apoptotic cells, dead cells, and necrotic cells in EAC are shown in **Fig. 5A, 5B**, and **5C.**
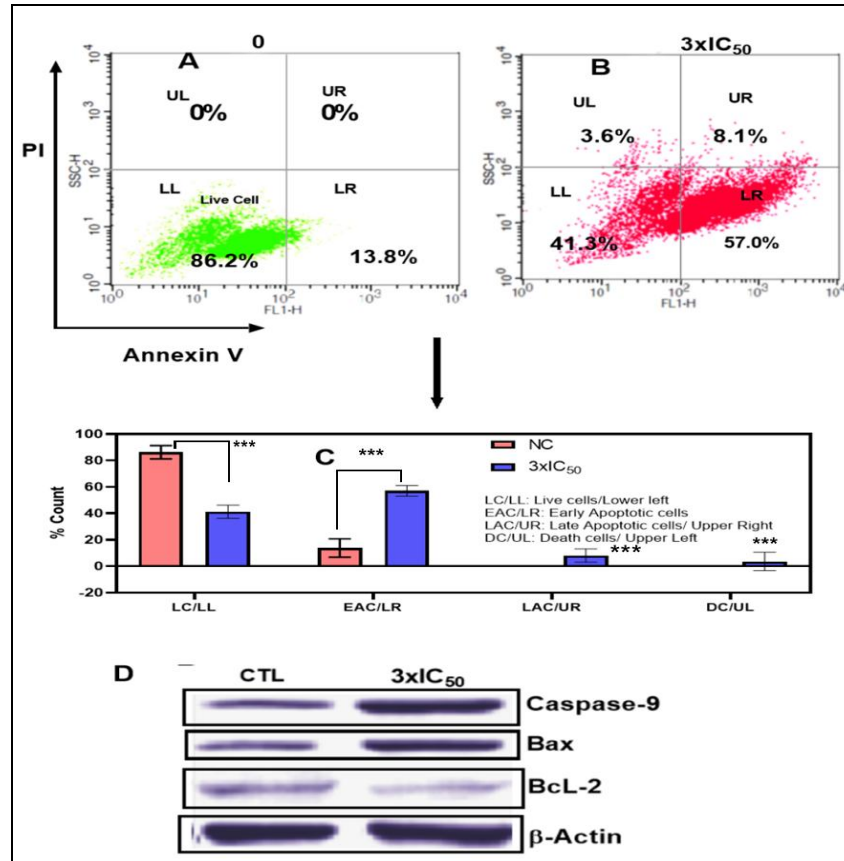

FIG. 5. (A-B): USING FLOW CYTOMETRY, THE IMPACT OF POP ON TRIGGERING APOPTOSIS IN EAC CELLS WAS ASSESSED. CELL CYCLE PHASE ANALYSIS WAS PERFORMED ON EAC CELLS AFTER THEY HAD BEEN TREATED WITH POP FOR 24 HOURS. THE PERCENTAGES OF LIVING CELLS, EARLY-PHASE APOPTOTIC CELLS, DEAD CELLS, AND NECROTIC CELLS IN EAC ARE SHOWN IN FIGURES 5A AND 5B. AFTER A 24-HOUR INCUBATION PERIOD, 86.2% OF THE CELLS IN THE CONTROL GROUP (5A) WERE FOUND TO BE VIABLE, 13.8% TO BE EXPERIENCING EARLY APOPTOSIS, AND NO CELLS WERE FOUND TO BE DEAD OR IN THE LATE APOPTOTIC STAGE. ON THE OTHER HAND, (5B) EAC CELLS TREATED WITH POP AT 3XIC50 SHOWED A UNIQUE PROFILE: 41.3% OF THE CELLS WERE LIVING, 57% WERE IN THE EARLY APOPTOTIC STAGE, 3.6% WERE DEAD, AND 8.1% WERE IN THE LATE APOPTOTIC STAGE.THESE FINDINGS HIGHLIGHT THE NOTICEABLE IMPACT OF POP TREATMENT ON BOTH CELL VIABILITY AND APOPTOTIC PROCESSES WITHIN THE EXPERIMENTAL MODEL. (C): WITH A SIGNIFICANCE THRESHOLD OF P < 0.05, THE GRAPHICAL REPRESENTATIONS OF A AND B OFFER COMPREHENSIVE STATISTICAL COMPARISONS BETWEEN THE TREATMENT GROUP (TREATED WITH 3XIC50) AND THE CONTROL GROUP (NC). COMPREHENSIVE STUDIES OF MANY PARAMETERS OR RESULTS, SUCH AS POP-INDUCED APOPTOSIS OF EAC CELLS, ARE COMPARED ACROSS FOUR QUADRANTS: DC/UL (UPPER LEFT), EAC/LR (LOWER RIGHT), LC/LL (LOWER LEFT), AND LAC/UR (UPPER RIGHT). (D) THE STUDY'S EXPRESSION ANALYSIS REVEALED SIGNIFICANT CHANGES IN THE AMOUNTS OF PROTEINS IN THE TREATED EAC CELLS. IN PARTICULAR, THERE WAS A NOTICEABLE DECLINE IN THE EXPRESSION OF THE BCL-2 PROTEIN, WHICH IS RECOGNISED FOR ITS ANTI-APOPTOTIC PROPERTIES AND MAY SUGGEST A CHANGE IN FAVOUR OF INDUCING APOPTOSIS. IN CONTRAST, THERE WAS A DISCERNIBLE RISE IN THE EXPRESSION LEVELS OF THE PRO-APOPTOTIC PROTEIN BAX AND THE CRUCIAL CASPASE INITIATOR CASPASE-9, WHICH IS IMPLICATED IN THE SIGNALLING PATHWAYS LEADING TO APOPTOSIS. THESE RESULTS POINT TO A REGULATORY MECHANISM THAT PROMOTES APOPTOSIS IN EAC CELLS BY DOWNREGULATING ANTI-APOPTOTIC PROTEINS (BCL-2) AND UPREGULATING PRO-APOPTOTIC FACTORS (BAX AND CASPASE-9). Each point, three independent experiments were carried out, and typical findings were displayed. the data shows the three experiments' mean ± sd. relative to the control group, *p<0.05, **p<0.01 signify statistical significance.

After a 24-hour incubation period, the control group exhibited a cell viability of 86.2%, with 13.8% undergoing early apoptosis. Notably, no cells were observed in a dead or late apoptotic state. In contrast, EAC cells treated with POP at $3xIC_{50}$ presented a distinct profile, featuring 41.3% live cells, 57% in the early apoptotic stage, 3.6% identified as dead cells, and 8.1% in the late apoptotic stage. This analysis underscores the discernible impact of POP treatment on both cell viability and apoptotic processes in the experimental context. The intrinsic apoptosis pathway, predominantly regulated by mitochondria, [38-39] was investigated to discern its involvement in POP-induced apoptosis. When EAC cells were treated with 3xIC50 POP, analysis of the Bcl-2 family proteins showed overexpression of pro-apoptotic Bax and downregulation of anti-apoptotic Bcl-2, indicating mitochondrial engagement **Fig. 5D.** p53 proteins may have an effect on the dysregulation of Bcl-2 and Bax protein production, which is a crucial mechanism governing the fate of cells during apoptosis [40]. Western blot analysis further demonstrated elevated p53 levels post-POP treatment, suggesting activation of the p53 pathway in response to POP-induced stress **Fig. 7D**. Additionally, the appearance of cleaved caspase-9 confirmed apoptosis induction by POP **Fig. 7D**.

These findings underscore the significance of the mitochondrial apoptotic pathway in POP-induced apoptosis in EAC cells, advancing our understanding of POP's anti-cancer effects.

Effect of POP on DNA Fragmentation and Caspase Activity: Caspase-9 activation precedes DNA fragmentation in apoptosis. It acts as a key initiator, triggering downstream caspase activation, including caspase-3, leading to DNA fragmentation and other apoptotic changes [41]. A DNA fragmentation experiment was performed on treated cells to determine whether apoptosis-mediated DNA fragmentation plays a role in POP-induced cell death. The findings, which are displayed in **Fig. 6A**, demonstrated a distinctive laddering pattern of broken DNA, suggestive of internucleosomal DNA degradation, a defining trait of apoptosis. The activity of caspase 9, a crucial modulator of the intrinsic apoptotic pathway, was assessed in order to provide insights into the molecular process underlying apoptosis triggered by POP **Fig. 5D**. Comparing POP-treated cells to untreated cells (CTL), **Fig. 6B** shows a substantial increase in caspase 9 activity. These results imply that POP induces apoptosis *via* the intrinsic route, which involves caspase 9 activation.
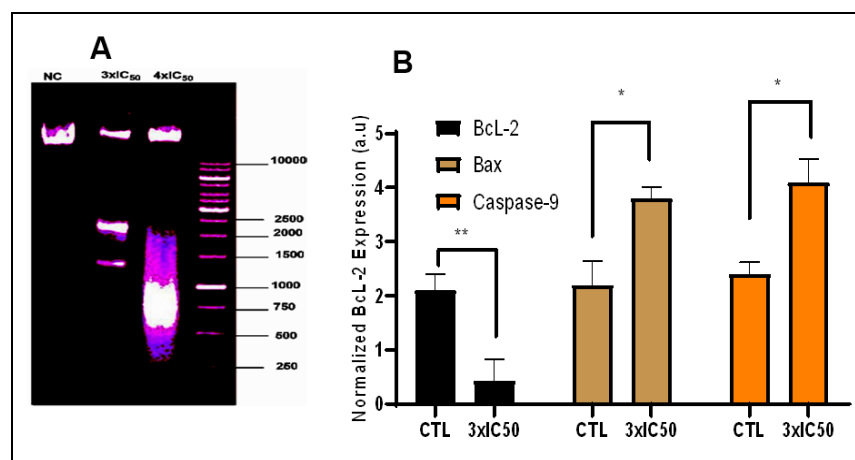

FIG. 6: EXAMINATION OF THE EXPRESSION OF APOPTOTIC PROTEINS AND DNA FRAGMENTATION. (A) The results, which are shown in Figure 6A, revealed a ladder-like pattern of DNA fragmentation at 3xIC50 and 4xIC50 concentrations, which is suggestive of internucleosomal DNA degradation, a hallmark feature of apoptosis. In order to investigate the molecular processes behind POP-induced apoptosis, caspase 9, a crucial modulator of the intrinsic apoptotic pathway, was evaluated (Figure 5D). (B) As compared to the untreated control (CTL), Figure 6B shows a significant increase in caspase 9 activity in POP-treated cells. These findings clearly imply that POP triggers apoptosis through the intrinsic route, which involves caspase 9 activation. The data on protein activity are shown as the means ± standard deviations from three separate experiments. Significant deviations from the control at $*P \leq 0.05()$ or $**P \leq 0.01$ are indicated by bars with asterisks.

Effect of POP on Cell Cycle Arrest: In addition to apoptosis, blocking cell cycle progression is

crucial for controlling cancer cell growth. Cancer cells often have abnormal cell cycle regulation,

leading to uncontrolled proliferation. Targeting key cell cycle regulators like cyclins and CDKs can slow down cell division [42]. Flow cytometry was utilised in the examination of cell cycle arrest to evaluate the distribution of EAC cells at different stages of the cell cycle after POP treatment at 3xIC50. EAC cells were primarily found in the G0/G1 phase in the control group, with populations

in the G2/M and S phases following. On the other hand, G2/M and S phase populations significantly decreased after POP therapy, whereas G0/G1 populations simultaneously increased. This change in cell cycle distribution raises the possibility that POP therapy, particularly during the G0/G1 phase, may obstruct cell cycle progression.
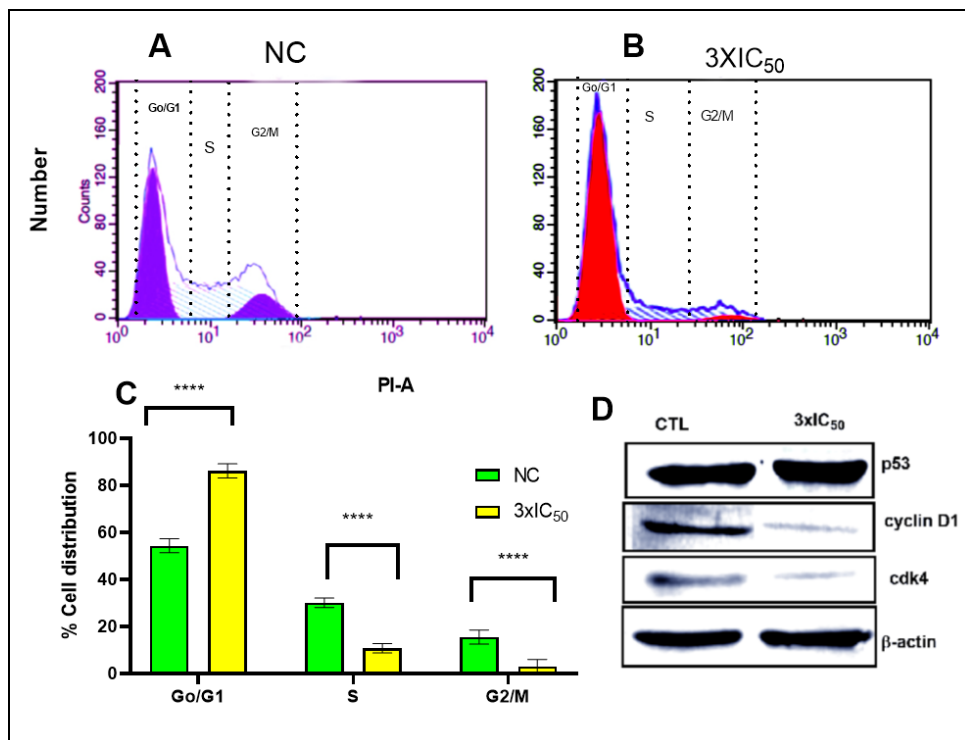

FIG. 7. (A–B): AFTER TREATING EAC CELLS WITH POP AT 3XIC50, THE DISTRIBUTION OF THESE CELLS ACROSS THE VARIOUS CELL CYCLE STAGES WAS ASSESSED USING FLOW CYTOMETRY TO ANALYSE CELL CYCLE ARREST. EAC CELLS WERE PRIMARILY IDENTIFIED IN THE G0/G1 PHASE IN THE CONTROL GROUP, WITH POPULATIONS IN THE G2/M AND S PHASES FOLLOWING. BUT AFTER POP THERAPY, THERE WAS A SIGNIFICANT DROP IN G2/M AND S PHASE POPULATIONS ALONG WITH A SIMULTANEOUS RISE IN G0/G1 POPULATIONS. THE OBSERVED CHANGE IN THE DISTRIBUTION OF THE CELL CYCLE IMPLIES THAT POP THERAPY MAY HINDER THE PROGRESSION OF THE CELL CYCLE, ESPECIALLY DURING THE G0/G1 PHASE. (B) THE STATEMENT SHOWS THAT WHEN POP IS ADMINISTERED AT THREE TIMES THE IC50 CONCENTRATION (3XIC50) COMPARED TO THE CONTROL CONDITION (NC), THERE ARE NOTABLE CHANGES IN THE PERCENTAGE DISTRIBUTION OF CELLS ACROSS THE G0/G1, S, AND G2/M STAGES OF THE CELL CYCLE. A STATISTICALLY SIGNIFICANT DIFFERENCE (P<0.05) IN THE CELL DISTRIBUTION BETWEEN THE TWO CONDITIONS IS SEEN IN EVERY STEP. IN PARTICULAR, AFTER RECEIVING POP TREATMENT, THERE IS A NOTICEABLE SHIFT IN THE PROPORTION OF CELLS IN THE G0/G1 PHASE, S PHASE, AND G2/M PHASE AS COMPARED TO THE CONTROL CONDITION. THESE RESULTS DEMONSTRATE THE EFFECT OF POP THERAPY ON THE CONTROL OF CELL CYCLE DYNAMICS IN EAC CELLS BY INDICATING THAT IT CAUSES MODIFICATIONS IN CELL CYCLE PROGRESSION THAT MAY HINDER CELL DIVISION AND PROLIFERATION. (D) IN ORDER TO INVESTIGATE THE EXPRESSION LEVELS OF IMPORTANT REGULATORY PROTEINS CONNECTED TO THE G0/G1 PHASE, SPECIFICALLY P53, CYCLIN D, AND CDK4, WE USED WESTERN BLOT ANALYSIS. THE FINDINGS SHOWED THAT P53 EXPRESSION HAD INCREASED WHEREAS CYCLIN D AND CDK4 LEVELS HAD DECREASED. THESE RESULTS ARE IN LINE WITH THE FLOW CYTOMETRIC STUDY, WHICH SHOWED THAT THE G0/G1 PHASE WAS ARRESTED.

As seen in **Fig. 7A–7B**, the observed alterations in cell cycle phases point to a possible regulatory

influence of POP on the cell cycle dynamics in EAC cells. By assessing the expression of key

regulatory proteins associated with the G0/G1 phase, namely p53, Cyclin D, and Cdk4, we used Western blot analysis to confirm the halted phase of the cell cycle. Cyclin D and Cdk4 were shown to be downregulated in conjunction with an increase of p53. This is consistent with the flow cytometric data **Fig. 7D** showing G0/G1 phase arrest.

DISCUSSION: Consuming medicinal or edible mushrooms is linked to improved human health, particularly in cancer prevention [43]. The active ingredients in mushrooms, known as polysaccharides, are thought to be the cause of these health advantages since they have been demonstrated to cause tumour cell death in a number of cancer types [44]. Numerous chemical compounds display cytotoxicity against cancer cells, presenting opportunities for anticancer therapy. However, their lack of selectivity often results in harmful effects on healthy cells, leading to adverse side effects. Conversely, polysaccharides extracted from a variety of sources, including plants, fungi, algae, and animals, have emerged as promising candidates for antitumor therapy due to their unique characteristics. These polysaccharides offer inherent advantages such as biocompatibility, biodegradability, and low toxicity to normal cells [45-49]. Research indicates that polysaccharides demonstrate cytotoxic effects against cancer cells while sparing healthy cells, providing a promising avenue for cancer treatment with reduced adverse effects. The distinctive structural and functional properties of polysaccharides enable them to selectively target cancer cells, often through mechanisms involving apoptosis induction, cell cycle arrest, and immunomodulation. Furthermore, polysaccharides may enhance the body's immune response against cancer cells, enhancing their potential as effective antitumor agents [50-53].

In this work, we used ion-exchange and gel filtration chromatography to separate the polysaccharide (POP) from the *Pleurotus ostreatus* fruiting bodies. We used an integrated FT-IR, GC-MS, and NMR spectroscopic investigation strategy to decipher the structural properties of POP. This multifaceted analysis framework serves as the foundation for deciphering the molecular architecture of POP. FT-IR spectroscopy provided insights into the functional groups present in POP

Fig. 1A. Peaks at specific wavenumbers indicated the presence of characteristic bonds, such as –OH groups, C-H bonds, and C=O bonds. Moreover, the presence of β-glycosidic linkages, confirmed by peaks in the 990-1050 cm-1 range, indicated the main chain of the polysaccharide to be α-D-glucopyranose. The retention time and mass spectrograms of PMAA were utilized for identifying the glycosylation linkage of POP. Methylation analysis further elucidated the glycosyl linkages present in POP **Fig. 1B** and **Table 1**, revealing specific methylated sugars and their molar ratios. This detailed analysis offers valuable information on the glycosylation patterns and overall structural composition of POP.

The NMR spectra of POP are depicted in **Fig. 2C** and 2D, with detailed data provided in Table 2. In the ^1H NMR spectrum, the chemical shift range of heterocephalic hydrogen signals from POP was below 5 ppm, indicating the presence of β-configurations. Additionally, this conclusion was corroborated by the chemical shift peaks observed between 102–112 ppm in the ^{13}C NMR spectrum. The absence of a signal peak at 5.40 ppm suggested that POP consisted of pyranose, consistent with the findings from FT-IR analysis. The ^{13}C NMR signals of POP predominantly fell within the range of 170–20 ppm, corresponding to the C1–C6 carbon atoms **Table 2**.

Beyond structural analysis, the MTT assay was used to assess the cytotoxicity of POP against Ehrlich Ascites Carcinoma (EAC) cells **Fig. 3**. POP exhibited significant cytotoxic activity, with an IC_{50} value indicating its potency against cancer cells. Polysaccharides applied in the study exhibited dose-dependent cytotoxicity against cancer cells. Within the dosage range of 25 to 800 µg/mL, POP showed significant antitumor activity against EAC tumor cells. At 121.801 µg/mL, it achieved a 50.0% inhibition rate [54-56].Our findings reveal that POP is a key active ingredient contributing to the anticancer properties of *Pleurotus ostreatus*, making it a promising candidate for cancer therapy. The anti-cancer efficacy of natural polysaccharides is closely linked to their molecular weight and monosaccharide composition. A recent study highlighted that polysaccharides with higher molecular weights demonstrated significant inhibitory effects against

S-180 tumor cells [57]. In *Pleurotus ostreatus*, various polysaccharides including β-glucans, α-glucans, and heteropolysaccharides have been identified and investigated for their diverse biological activities. The molecular weights of these polysaccharides can vary significantly, ranging approximately from 100,000 Da to over 1,000,000 Da, influenced by factors such as extraction methods and fungal strains. Specifically, α-glucans and heteropolysaccharides exhibit similar variability. Numerous investigations have demonstrated that the molecular weight (Mw) of polysaccharides has a critical role in their biological activities [58-62].

Despite the potential therapeutic benefits attributed to natural polysaccharides with large molecular masses, uncertainties persist regarding their ability to penetrate the bloodstream and exert anticancer effects. This ambiguity is underscored by the limited number of mushroom polysaccharides that have undergone rigorous clinical evaluation in humans, as evidenced by existing literature [63]. Furthermore, new data indicates that the majority of mushroom polysaccharides with significant anti-tumor effect are heteropolysaccharides, [64], further complicating our understanding of their biological mechanisms and therapeutic potential.

Our investigation examined the structural properties and anticancer activity of polysaccharides obtained from *Pleurotus ostreatus* (POP) in accordance with these findings. Our findings corroborate previous reports, demonstrating that POP, with its highest observed molecular weight of 1.5×10^5 Da, predominantly comprises a homopolysaccharide, accounting for 98.4% of the total sugar content, alongside a minor protein fraction of 1.6%. Notably, this structural composition mirrors our previous investigations and highlights POP as the polysaccharide variant with the most potent antitumor activity within the *Pleurotus ostreatus* species. The observed efficacy of POP in inhibiting the proliferation of EAC cells can be attributed to its unique structural features. Specifically, the high molecular weight and homopolymeric nature of POP likely contribute to its enhanced bioactivity, facilitating interactions with cellular targets implicated in cancer progression. Furthermore, the substantial sugar content coupled with a minor protein component

underscores the importance of polysaccharide purity and composition in dictating biological activity. The antitumor effects of polysaccharides from *Pleurotus ostreatus* (POP) were investigated across various phenotypic attributes of EAC cells, providing insights into their potential mechanisms of action. These phenotypic traits included colony formation, metastatic potential, and migration abilities, as evidenced by the results presented in **Fig. 4A-4F**. Colony formation is a critical characteristic of cancer cells, reflecting their ability to rapidly proliferate and form clusters, which can contribute to tumor growth and progression. Metastasis, on the other hand, represents the spread of cancer cells from the primary tumor to distant sites in the body, a process associated with increased morbidity and mortality in cancer patients [65-67].

The observed results in Figure 4 highlight the susceptibility of EAC cell lines to the antitumor effects of polysaccharides derived from *Pleurotus ostreatus.* This suggests that POP may exert inhibitory effects on key processes involved in tumor progression, including colony formation and metastasis. The capacity of cancer cells to spread and infiltrate neighbouring tissues is a fundamental aspect of metastasis [68-70]. According to the results shown in **Fig. 4**, applied polysaccharides reduced cancer cells' ability to migrate and invade in a dose-dependent way. This shows that POP may act through processes regulating cell adhesion, motility, and metastasis-related signalling pathways to inhibit the ability of cancer cells to propagate.

In order to investigate the fundamental mechanism underlying the cell death caused by polysaccharides derived from *Pleurotus ostreatus* (POP), we utilised a technique that entailed double-label staining using PI and annexin-V, succeeded by flow cytometry analysis. Phosphatidylserine (PS), a lipid that is typically found on the inner side of the plasma membrane in healthy cells, is the specific target of annexin-V binding, which inhibits annexin-V binding in normal conditions. But in the initial phases of apoptosis, PS translocates to the outer membrane, which makes it possible for annexin-V to attach to PS specifically and recognise apoptotic cells [71-72]. As apoptosis progresses, both apoptotic and necrotic cells stain positively due to dye penetration into the nucleus,

where they bind to DNA [73-75]. Our flow cytometry results, as illustrated in Figure 5(A-C), revealed that POP induces cell death through apoptosis in a dose-dependent manner. After 24 hours, the control group showed 86.2% cell viability and 13.8% early apoptosis, while EAC cells treated with POP at 3xIC50 had 41.3% live cells, 57% early apoptotic, 3.6% dead, and 8.1% late apoptotic cells. Apoptosis, a programmed cell death process, is heavily influenced by mitochondria, making them promising targets for cancer therapy [76]. Bcl-2 family proteins have a role in mitochondrial-mediated apoptosis by counteracting pro-apoptotic factors like Bax and anti-apoptotic factors like Bcl-2. By focusing on mitochondria and Bcl-2 family proteins, this delicate balance offers hope for the development of cancer treatments by determining whether cells survive or undergo apoptosis.

The results of our study indicate that POP treatment may cause a shift in the ratio of pro-to anti-apoptotic Bcl-2 family proteins, which may then play a role in mitochondrial-mediated apoptosis. Specifically, Bax expression was upregulated and Bcl-2 expression was downregulated. The Bcl-2 protein family is involved in controlling the equilibrium between cell survival and death through the regulation of mitochondrial membrane permeability. This results in the reduction of mitochondrial transmembrane potential ($\Delta\Psi$m), an essential step in the apoptotic process [77-81]. Western blot analysis further confirmed the involvement of caspase-9 in POP-induced apoptosis in EAC cells, underscoring that POP triggers apoptosis through mitochondrial pathways.

On the other hand, DNA fragmentation and caspase-9 activation are key events in the process of apoptosis mediated by mitochondria. During apoptosis, various cellular changes occur, including the cleavage of genomic DNA into characteristic fragments. Apoptosis is characterised by DNA fragmentation, which is frequently preceded by the activation of caspase-9, an initiator caspase in the intrinsic or mitochondrial pathway of apoptosis [82-86]. We found strong evidence supporting the idea that the observed cell death was mostly caused by apoptosis via mitochondrial pathways based on our extensive analysis of DNA fragmentation **Fig. 4A** and caspase 9 enzyme activation **Fig. 4B**. In addition, flow cytometry revealed that POP caused

G0/G1 phase cell cycle arrest, and Western blot analysis corroborated this finding by displaying alterations in the expression of cell cycle regulatory proteins. This suggests a process by which POP causes cell cycle disruption and proliferation hindrance as part of its cytotoxic effects. Reduced G2/M and S phase populations as well as higher G0/G1 populations were found in POP-treated EAC cells at 3xIC50 flow cytometry analysis, compared to controls. This suggests that cell cycle progression is inhibited at G0/G1 **Fig. 7A-B** [87-89]. Bax creates pores in the mitochondrial membrane, which compromises its integrity and releases cytochrome c. BH-3 members increase the activation of Bax while blocking the antiapoptotic signal Bcl-2, which ultimately results in cell death [90-94].

In addition to inducing cell cycle arrest, p53 also directly causes abnormalities in the mitochondria. The results of the study showed that POP treatment increased the expression of Bax and p53 and decreased the expression of Bcl-2 in EAC cells, suggesting that p53 plays a role in POP-induced apoptosis. This indicates that the treatment's effectiveness in inducing apoptosis is influenced by this balance between proapoptotic and antiapoptotic genes. These findings underscore that POP induces apoptosis by modulating the expression of these genes, ultimately shifting the balance towards apoptosis.

In summary, the structural characterization of *Pleurotus ostreatus* polysaccharide (POP) through UV-Viz, FT-IR, and NMR techniques provides crucial insights into its composition and properties, confirming the removal of protein and nucleic acids and revealing characteristic functional groups and glycosidic linkages, indicative of its structural integrity. Additionally, cytotoxicity testing on Ehrlich Ascites Carcinoma (EAC) cells reveals that POP has strong anticancer properties, including the ability to prevent cell migration, invasion, and colony formation as well as to induce cell cycle arrest and apoptosis. These results underline POP's potential as a potent anti-cancer therapeutic agent, calling for more research and development of clinical uses.

Funding: The authors did not receive support from any organization for the submitted work.

Contributions: MPK conducted compound isolation and activity assays, with support from JO and MSI for structure elucidations. LA and RP were responsible for sample collection. MPK authored and designed the manuscript, which was reviewed by MR and MSB. All authors provided comments and approved the final version.

CONFLICTS OF INTEREST: All authors affirm that there are no conflicts of interest.

REFERENCES:

1. Jemal A, Bray F, Center MM, Ferlay J, Ward E and Forman D: Global cancer statistics. CA Cancer J Clin 2011; 61: 69-90.
2. Moussavou G, Kwak DH, Obiang-Obonou BW, Maranguy CA, Dinzouna-Boutamba SD and Lee DH: Anticancer effects of different seaweeds on human colon and breast cancers. Mar Drugs 2014; 12: 4898-911.
3. Hosseini B-A, Pasdaran A, Kazemi T, Shanehbandi D, Karami H and Orangi M: Dichloromethane fractions of Scrophulariaoxysepala extract induce apoptosis in EAChuman breast cancer cells. Bosn J Basic Med Sci 2015; 15: 26-32
4. Aghbali A, Hosseini SV, Delazar A, Gharavi NK, Shahneh FZ and Orangi M: Induction of apoptosis by grape seed extract (Vitis vinifera) in oral squamous cell carcinoma. Bosn J Basic Med Sci 2013; 13: 186-91.
5. Meng X, Liang H and Luo L: Antitumor polysaccharides from mushrooms: a review on the structural characteristics, antitumor mechanisms and immunomodulating activities. Carbohydr Res 2016; 424: 30-41.
6. Pk MMU, O'Sullivan J, Pervin R and Rahman M: Antioxidant of *Pleurotus ostreatus* (Jacq.) P. Kumn and lymphoid cancer cells. In: Preedy VR, Patel VB, editors. Cancer (Second Edition). San Diego: Academic Press 2021; 427-37.
7. Shi JJ, Zhang JG, Sun YH, Qu J, Li L and Prasad C: Physicochemical properties and antioxidant activities of polysaccharides sequentially extracted from peony seed dreg. Int J Biol Macromol 2016; 91: 23-30.
8. Li N, Li L, Fang J, Wong J, Ng T and Jiang Y: Isolation and identification of a novel polysaccharide-peptide complex with antioxidant, anti-proliferative and hypoglycaemic activities from the abalone mushroom. Bioscience reports 2011; 32: 221-8.
9. Friedman M: Mushroom Polysaccharides: Chemistry and Antiobesity, Antidiabetes, Anticancer, and Antibiotic Properties in Cells, Rodents, and Humans. Foods 2016; 5: 80.
10. Uddin Pk MM, Islam MS, Pervin R, Dutta S, Talukder RI and Rahman M: Optimization of extraction of antioxidant polysaccharide from *Pleurotus ostreatus* (Jacq.) P. Kumm and its cytotoxic activity against murine lymphoid cancer cell line. PLOS ONE 2019; 14: 0209371.
11. Vafaee K, Dehghani S, Tahmasvand R, Saeed Abadi F, Irian S and Salimi M: Potent antitumor property of *Allium bakhtiaricum* extracts. BMC Complementary and Alternative Medicine 2019; 19: 116.
12. Chen J, Chen J, Wang X and Liu C: Anti-tumour effects of polysaccharides isolated from *Artemisia annua* L by inducing cell apoptosis and immunomodulatory anti-hepatoma effects of polysaccharides. Afr J Tradit Complement Altern Med 2013; 11: 15-22.
13. Gao Y, Gao H, Chan E, Tang W, Xu A and Yang H: Antitumor activity and underlying mechanisms of ganopoly, the refined polysaccharides extracted from *Ganoderma lucidum*, in mice. Immunol Invest 2005; 34: 171-98.
14. Wang J, Hu Y, Wang D, Liu J, Zhang J and Abula S: Sulfated modification can enhance the immune-enhancing activity of lyciumbarbarum polysaccharides. Cell Immunol 2010; 263: 219-23.
15. Manzi P, Gambelli L, Marconi S, Vivanti V and Pizzoferrato L: Nutrients in edible mushrooms: an inter-species comparative study. Food Chem 1999; 65: 477-482.
16. Wang JC, Hu SH, Liang ZC and Yeh CJ: Optimization for the production of water-soluble polysaccharide from *Pleurotus citrinopileatus* in submerged culture and its antitumor effect. Appl Microbiol Biotechnol 2005; 67: 759-66.
17. Bobek P, Nosálová V and Cerná S: Effect of pleuran (beta-glucan from *Pleurotus ostreatus*) in diet or drinking fluid on colitis in rats. Nahrung 2001; 45: 360-3.
18. Zhuang C, Mizuno T, Shimada A, Ito H, Suzuki C, Mayuzumi Y, Okamoto H, Ma Y and Li J: Antitumor protein-containing polysaccharides from a Chinese mushroom Fengweigu or Houbitake, *Pleurotus sajor-caju* (Fr.) Sings. Biosci Biotechnol Biochem 1993; 57: 901-6.
19. Yoshioka Y, Tabeta R, Saitô H, Uehara N and Fukuoka F: Antitumor polysaccharides from *P. ostreatus* (Fr.) Quél.: isolation and structure of a beta-glucan. Carbohydr Res 1985; 140: 93-100.
20. Jose N and Janardhanan KK: Antioxidant and antitumour activity of *Pleurotus florida*. Curr Sci India 2001; 79: 941–943.
21. Li N, Li L, Fang JC, Wong JH, Ng TB and Jiang Y: Isolation and identification of a novel polysaccharide-peptide complex with antioxidant, anti-proliferative and hypoglycaemic activities from the abalone mushroom. Biosci Rep 2012; 32: 221-8.
22. Li X, Wang Z, Wang L, Walid E and Zhang H: *In-vitro* antioxidant and anti-proliferation activities of polysaccharides from various extracts of different mushrooms. Int J Mol Sci 2012; 13: 5801-5817.
23. Lowry OH, Rosebrough NJ, Farr AL and Randall RJ: Protein measurement with the Folin phenol reagent. J Biol Chem 1951; 193: 265-75.
24. Jain VM, Karibasappa GN, Dodamani AS and Mali GV: Estimating the carbohydrate content of various forms of tobacco by phenol-sulfuric acid method. J Educ Health Promot 2017; 6: 90.
25. Li X, Zhao R, Zhou HL and Wu DH: Deproteinization of Polysaccharide from the Stigma Maydis by Sevag Method. Advanced Materials Research 2012; 340: 416-20.
26. Wu Q, Luo M, Yao X and Yu L: Purification, structural characterization, and antioxidant activity of the COP-W1 polysaccharide from Codonopsistangshen Oliv. Carbohyd Polym 2020; 236: 116020.
27. Zhang H, Zhang M, Yu L, Zhao Y, He N and Yang X: Antitumor activities of quercetin and quercetin-5',8-disulfonate in human colon and breast cancer cell lines. Food Chem Toxicol 2012; 50: 1589-99.

28. Chidambara Murthy KN, Jayaprakasha GK, Kumar V, Rathore KS and Patil BS: *Citrus limonin* and its glucoside inhibit colon adenocarcinoma cell proliferation through apoptosis. J Agric Food Chem 2011; 59: 2314-23.

29. Arnott S, Scott WE, Rees DA and McNab CG: Iota-carrageenan: molecular structure and packing of polysaccharide double helices in oriented fibres of divalent cation salts. J Mol Biol 1974; 90: 253-67.

30. Justus CR, Leffler N, Ruiz-Echevarria M and Yang LV: *In-vitro* cell migration and invasion assays. J Vis Exp 2014; 88: 51046.

31. Ma L, Teruya-Feldstein J and Weinberg RA: Tumour invasion and metastasis initiated by microRNA-10b in breast cancer. Nature 2007; 449: 682-8.

32. Franken NA, Rodermond HM, Stap J, Haveman J and van Bree C: Clonogenic assay of cells *in-vitro*. Nat Protoc 2006; 1: 2315–9.

33. Looi CY, Imanishi M, Takaki S, Sato M, Chiba N and Sasahara Y: Octa-arginine mediated delivery of wild-type Lnk protein inhibits TPO-induced M-MOK megakaryoblastic leukemic cell growth by promoting apoptosis. PLoSOne 2011; 6: 23640.

34. Looi CY, Arya A, Cheah FK, Muharram B, Leong KH and Mohamad K: Induction of Apoptosis in Human Breast Cancer Cells *via* Caspase Pathway by Vernodalin Isolated from *Centratherum anthelminticum* (L.) Seeds. PLOSONE 2013; 8: 56643.

35. Mahmoud R. Hussein, Mohamed A. Bedaiwy and Tommaso Falcone: Analysis of apoptotic cell death, Bcl-2, and p53 protein expression in freshly fixed and cryopreserved ovarian tissue after exposure to warm ischemia. Fertility and Sterility 2006; 85: 1082-1092.

36. van Zijl F, Krupitza G and Mikulits W: Initial steps of metastasis: cell invasion and endothelial transmigration. Mutat Res 2011; 728: 23-34.

37. Wyllie AH: Cell death: a new classification separating apoptosis from necrosis. Cell death in biology and pathology. Dordrecht: Springer Netherlands 1981; 9-34.

38. Denicourt C, Dowdy SF and Medicine: Targeting apoptotic pathways in cancer cells. Science 2004; 305: 1411-3.

39. Li Y, Liu J and Li Q: Mechanisms by which the antitumor compound di-n-butyl-di-(4-chlorobenzohydroxamato)tin (IV) induces apoptosis and the mitochondrial-mediated signaling pathway in human cancer SGC-7901 cells. Mol Carcinog 2010; 49: 566-81.

40. Qiu P, Guan H, Dong P, Li S, Ho CT and Pan MH: The p53-, Bax- and p21-dependent inhibition of colon cancer cell growth by 5-hydroxy polymethoxyflavones. Mol Nutr Food Res 2011; 55: 613-22.

41. McIlwain DR, Berger T and Mak TW: Caspase functions in cell death and disease. Cold Spring Harb Perspect Biol 2013; 5: 008656.

42. Qiu P, Guan H, Dong P, Li S, Ho CT and Pan MH: The p53-, Bax- and p21-dependent inhibition of colon cancer cell growth by 5-hydroxy polymethoxyflavones. Mol Nutr Food Res 2011; 55: 613-22.

43. Zhang M, Cui SW, Cheung PCK and Wang Q: Antitumor polysaccharides from mushrooms: a review on their isolation process, structural characteristics and antitumor activity. Trends Food Sci Tech 2007; 18: 4–19.

44. Ko HG, Park HG, Park SH, Choi CW, Kim SH and Park WM: Comparative study of mycelial growth and basidiomata formation in seven different species of the edible mushroom genus Hericium. Bioresour Technol 2005; 96: 1439-44.

45. Wang J, Wang W & Liu J: Polysaccharides as anticancer agents: a review. Carbohydrate Polymers 2020: 241: 116364.

46. Wu, DT & Liu W: Polysaccharides from *Pleurotus ostreatus* induce apoptosis in lung cancer cells via a mitochondrial pathway. International Journal of Biological Macromolecules 2019; 123: 233-239.

47. Jiao L, Zhang X, Li, H & Wang Z: The anti-tumor effect of polysaccharides from Lentinus edodes on gastric cancer. International Journal of Biological Macromolecules 2019; 122: 328-334.

48. Zhang Q & Wang J: Polysaccharides from Ganoderma lucidum attenuate microglia-mediated neuroinflammation and modulate microglial phagocytosis and behavioural response. Journal of Neuroinflammation 2019; 16: 1-13.

49. Chen J & Wang W: Biological activities and potential health benefits of polysaccharides from Cordyceps fungi: A review. Food Hydrocolloids 2020; 112: 106350.

50. Chen J, Wei X, Wang G & Fan Y: Structural characterization and antitumor activity of polysaccharides from Lentinula edodes. International Journal of Biological Macromolecules 2020; 145: 1243-1252.

51. Li W, Luo Y & Lu L: Polysaccharides from *Ganoderma lucidum* ameliorate the immune dysfunction in induced by cyclophosphamide in mice. International Journal of Biological Macromolecules 2019; 121: 874-881.

52. Zhang J, Zhang Q, Li Y & Wang X: Structural characterization and antitumor activity of polysaccharides from *Lycium barbarum*. International Journal of Biological Macromolecules 2020; 146: 904-912.

53. Wang C, Shi L, Ren H & Xu Q: Structural characterization and antitumor activity of polysaccharides from *Phellinus igniarius*. International Journal of Biological Macromolecules 2019; 125: 840-849.

54. Khinsar KH, Abdul S, Hussain A. Wang L and Mintao Z: Anti-tumor effect of polysaccharide from *Pleurotus ostreatus* on H22 mouse Hepatoma ascites *in-vivo* and hepatocellular carcinoma *in-vitro* model. AMB Expr 2021; 11: 160.

55. Facchini JM, Alves EP, Aguilera C, Gern RM, Silveira ML and Wisbeck E: Antitumor activity of *Pleurotus ostreatus* polysaccharide fractions on Ehrlich tumor and Sarcoma 180. Int J Biol Macromol 2014; 68: 72-7.

56. Cao X, Liu J, Yang W, Hou X & Li Q: Antitumor activity of polysaccharide extracted from *Pleurotus ostreatus* mycelia against gastric cancer *in-vitro* and *in-vivo*. Molecular Medicine Reports 2015; 12: 2383-2389.

57. Chen X, Xu X, Zhang L and Zeng F: Chain conformation and anti-tumor activities of phosphorylated (1→3)-β-d-glucan from *Poria cocos*. Carbohyd Polym 2009; 78: 581–587.

58. Kim JH & Park S: Anti-inflammatory effect of high molecular weight chitosan in dextran sulfate sodium-induced colitis in mice. International Journal of Biological Macromolecules 2019; 122: 179-186.

59. Wang Y, Li Y, Zhang X, Liang J. Hu Y & Liu J: Effects of molecular weight and acidic groups of polysaccharides on antitumor activity and toxicity. Carbohydrate Polymers 2018; 183: 172-179.

60. Zhang Z, Wang X, Zhang J, Wang J and Li P: Effect of molecular weight of chitosan on antimicrobial activity against foodborne pathogens and spoilage bacteria. International Journal of Food Microbiology 2019; 296: 51-58.

61. Niu H, Wang Z, Zhao W, Wang J & Zhang Y: Structural characterization and immunomodulatory activity of low

molecular weight polysaccharides from *Hericium erinaceus*. Food & Function 2020; 11: 3217-3228.

62. Qi L, Xu Z, Chen S, Shi L & Yan H: Effects of molecular weight and chain conformation of polysaccharides on the antitumor activity of sea cucumber polysaccharides. Int J of Biological Macromolecules 2020; 162: 951-61.

63. Zong AZ, Cao HZ and Wang FS: Anticancer polysaccharides from natural resources: A review of recent research. Carbohyd Polym 2012; 90: 1395–1410.

64. Cooi VE and Liu F: Immunomodulation and anti-cancer activity of polysaccharide-protein complexes. Curr Med Chem 2000; 7: 715–729.

65. Zhang Y, Wang Z & Chen M: Regulation of cancer cell proliferation and metastasis by cell surface electrostatics. Trends in Cancer 2020; 6: 506-516.

66. Lambert AW, Pattabiraman DR & Weinberg RA: Emerging biological principles of metastasis. Cell 2017; 168: 670-691.

67. Taddei ML, Cavallini L, Comito G, Giannoni E & Folini M: Isolation and characterization of colon cancer stem cells from the colonosphere assay. Methods in Molecular Biology 2014; 1162: 235-246.

68. Friedl P and Alexander S: Cancer invasion and the microenvironment: plasticity and reciprocity. Cell 2011; 147: 992-1009.

69. Hanahan, Douglas and Robert A. Weinberg: Hallmarks of cancer: the next generation. Cell 2011; 144: 646-674.

70. Valastyan S and Weinberg RA: Tumor metastasis: molecular insights and evolving paradigms. Cell 2011; 147: 275-92.

71. Koopman G, Reutelingsperger CP, Kuijten GA, Keehnen RM, Pals ST and van Oers MH: Annexin V for flow cytometric detection of phosphatidylserine expression on B cells undergoing apoptosis. Blood 1994; 84: 1415-20.

72. Gasser SM and Raulet DH: The DNA damage response, immunity and cancer. Semin Cancer Biol 2006; 16: 344-7.

73. Vermes I, Haanen C, Steffens-Nakken H and Reutelingsperger C: A novel assay for apoptosis. Flow cytometric detection of phosphatidylserine expression on early apoptotic cells using fluorescein labelled Annexin V. J Immunol Methods 1995; 184: 39-51.

74. Martin SJ, Reutelingsperger CP, McGahon AJ, Rader JA, van Schie RC and LaFace DM: Early redistribution of plasma membrane phosphatidylserine is a general feature of apoptosis regardless of the initiating stimulus: inhibition by overexpression of Bcl-2 and Abl. J Exp Med. 1995; 182: 1545-56.

75. Van Engeland M, Nieland LJ, Ramaekers FC, Schutte B and Reutelingsperger CP: Annexin V-affinity assay: a review on an apoptosis detection system based on phosphatidylserine exposure. Cytometry 1998; 31: 1-9.

76. He N, Shi X, Zhao Y, Tian L, Wang D and Yang X: Inhibitory effects and molecular mechanisms of selenium-

containing tea polysaccharides on human breast cancer mcf-7 cells. J Agric Food Chem 2013; 61: 579–588.

77. Adams JM and Cory S: The Bcl-2 protein family: arbiters of cell survival. Science 1998; 281: 1322-6.

78. Kaufmann T, Strasser A and Jost PJ: Fas death receptor signalling: roles of Bid and XIAP. Cell Death Differ 2012; 19: 42-50.

79. Vander Heiden MG, Chandel NS, Williamson EK, Schumacker PT and Thompson CB: Bcl-xL regulates the membrane potential and volume homeostasis of mitochondria. Cell 1997; 91: 627-37.

80. Green DR and Kroemer G: The pathophysiology of mitochondrial cell death. Science 2004; 305: 626-9.

81. Kluck RM, Bossy-Wetzel E, Green DR and Newmeyer DD: The release of cytochrome c from mitochondria: a primary site for Bcl-2 regulation of apoptosis. Science 1997; 275: 1132-6.

82. Green DR and Reed JC: Mitochondria and apoptosis. Science 1998; 281: 1309-12.

83. Li P, Nijhawan D, Budihardjo I, Srinivasula SM, Ahmad M and Alnemri ES: Cytochrome c and dATP-dependent formation of Apaf-1/caspase-9 complex initiates an apoptotic protease cascade. Cell 1997; 91: 479-89.

84. Wang X: The expanding role of mitochondria in apoptosis. Genes Dev 2011; 15: 2922-33.

85. Jiang X and Wang X: Cytochrome C-mediated apoptosis. Annu Rev Biochem 2004; 73: 87-106.

86. Slee EA, Adrain C and Martin SJ: Executioner caspase-3, -6, and -7 perform distinct, non-redundant roles during the demolition phase of apoptosis. J Biol Chem 2001; 276: 7320-6.

87. Vousden KH and Prives C: Blinded by the light: the growing complexity of p53. Cell 2009; 137: 413-31.

88. Chipuk JE and Green DR: Dissecting p53-dependent apoptosis. Cell Death Differ 2006; 13: 994-1002.

89. Miyashita T and Reed JC: Tumor suppressor p53 is a direct transcriptional activator of the human bax gene. Cell 1995; 80: 293-9.

90. Chipuk JE and Green DR: How do BCL-2 proteins induce mitochondrial outer membrane permeabilization? Trends Cell Biol 2008; 18: 157-64.

91. Danial NN and Korsmeyer SJ: Cell death: critical control points. Cell 2013; 116: 205-19.

92. Green DR and Kroemer G: The pathophysiology of mitochondrial cell death. Science 2004; 305: 626-9.

93. Moll UM, Marchenko N and Zhang XK: p53 and Nur77/TR3 - transcription factors that directly target mitochondria for cell death induction. Oncogene 2006; 25: 4725-43.

94. Willis SN and Adams JM: Life in the balance: how BH3-only proteins induce apoptosis. Curr Opin Cell Biol 2005; 17: 617-25.